Author's Accepted Manuscript

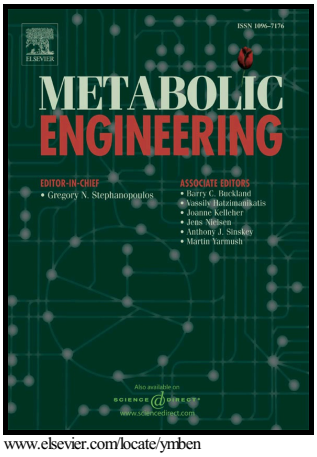

www.elsevier.com/locate/ymben

Efficient phototrophic production of a high-value sesquiterpenoid from the eukaryotic microalga *Chlamydomonas reinhardtii*

Kyle J. Lauersen, Thomas Baier, Julian Wichmann, Robin Wördenweber, Jan H. Mussgnug, Wolfgang Hübner, Thomas Huser, Olaf Kruse

PII: S1096-7176(16)30068-4
DOI: http://dx.doi.org/10.1016/j.ymben.2016.07.013
Reference: YMBEN1140

To appear in: *Metabolic Engineering*

Received date: 25 April 2016
Revised date: 17 June 2016
Accepted date: 26 July 2016

Cite this article as: Kyle J. Lauersen, Thomas Baier, Julian Wichmann, Robi Wördenweber, Jan H. Mussgnug, Wolfgang Hübner, Thomas Huser and Ola Kruse, Efficient phototrophic production of a high-value sesquiterpenoid fro the eukaryotic microalga *Chlamydomonas reinhardtii*, *Metabolic Engineerin* http://dx.doi.org/10.1016/j.ymben.2016.07.013

This is a PDF file of an unedited manuscript that has been accepted fo publication. As a service to our customers we are providing this early version o the manuscript. The manuscript will undergo copyediting, typesetting, an review of the resulting galley proof before it is published in its final citable form Please note that during the production process errors may be discovered whic could affect the content, and all legal disclaimers that apply to the journal pertain

ACCEPTED MANUSCRIPT

Efficient phototrophic production of a high-value sesquiterpenoid from the eukaryotic microalga Chlamydomonas reinhardtii

Kyle J. Lauersen[1], Thomas Baier[1], Julian Wichmann[1], Robin Wördenweber[1], Jan H. Mussgnug[1], Wolfgang Hübner[2], Thomas Huser[2], Olaf Kruse[1,*]

[1]Bielefeld University, Faculty of Biology, Centre for Biotechnology (CeBiTec), Universitätsstrasse 27, 33615, Bielefeld, Germany.
[2]Biomolecular Photonics, Department of Physics, Bielefeld University, Universitätsstr. 25, 33615, Bielefeld, Germany

[*]**Corresponding Author:** Olaf Kruse, Tel: +49 521 106-12258, fax: +49 521 106-12290. olaf.kruse@uni-bielefeld.de

Abstract

The heterologous expression of terpene synthases in microbial hosts has opened numerous possibilities for bioproduction of desirable metabolites. Photosynthetic microbial hosts present a sustainable alternative to traditional fermentative systems, using freely available (sun)light and carbon dioxide as inputs for bio-production. Here, we report the expression of a patchoulol synthase from Pogostemon cablin Benth in the model green microalga Chlamydomonas reinhardtii. The sesquiterpenoid patchoulol was produced from the alga and was used as a marker of sesquiterpenoid production capacity. A novel strategy for gene loading was employed and patchoulol was produced up to 922 ± 242 µg g^{-1} CDW in six days. We additionally investigated the effect of carbon source on sesquiterpenoid productivity from C. reinhardtii in scale-up batch cultivations. It was determined that up to 1.03 mg L^{-1} sesquiterpenoid products could be produced in completely photoautotrophic conditions and that the alga exhibited altered sesquiterpenoid production metabolism related to carbon source.

Keywords: Microalgae. Chlamydomonas reinhardtii. Terpenoids. Sesquiterpenoids. Patchoulol.

Abbreviations

PcPs – Pogostemon cablin Benth patchoulol synthase
TAP – Tris Acetate Phosphate medium

Accepted manuscript

ACCEPTED MANUSCRIPT

T2P – TAP medium without acetate and 2X phosphate content

FPP – farnesyl diphosphate

GPP – geranyl diphosphate

GGPP – geranylgeranyl diphosphate

CDW – Cell dry weight

YFP – mVenus yellow fluorescent protein

CFP – mCerulean3 cyan fluorescent protein

UQ – ubiquinone

1. Introduction

All domains of life exhibit the capacity to produce terpenoid compounds. Terpenoids, also known of as isoprenoids or terpenes, are a structurally diverse class of hydrocarbon molecules that serve numerous natural roles including, but not limited to, photoprotection, light-harvesting, defense, pigmentation, signalling, membrane fluidity, and electron transfer (Lange et al., 2000). Terpenes are classified by their respective number of carbon atoms (Kirby and Keasling, 2009): C10 monoterpenes, C15 sesquiterpenes, C20 diterpenes, C30 triterpenes, C40 tetraterpenes (carotenoids), and (C5)n with $n > 8$ polyterpenes. All terpenes are derived from the five carbon containing building blocks isopentenyl diphosphate (IPP) and dimethylallyl diphosphate (DMAPP), which are sequentially condensed by the diphosphate synthases (PPs, also known as prenyl transferases): geranyl diphosphate synthase to geranyl diphosphate (GPP, C10), farnesyl diphosphate synthase to farnesyl diphosphate (FPP, C15), and geranylgeranyl diphosphate synthase to geranylgeranyl diphosphate (GGPP, C20). These carbon precursors are rapidly converted into the vast diversity of known terpenoids by a class of enzymes known as terpene synthases, and the resulting hydrocarbon skeletons can be further modified, for example, by cyclization or addition of functional groups by cytochrome P450 enzymes (Pateraki et al., 2015; Weitzel and Simonsen, 2013).

Over 30,000 terpenoids have been described and characterized, representing one of the largest and oldest known classes of biological molecules (Buckingham et al., 1994). Terpenoid compounds are currently used in a variety of ways owing to their diverse chemical structures. Applications for terpenoids include medicine (Gershenzon and Dudareva, 2007; Nosten and White, 2007), natural flavouring (Beekwilder et al., 2014), platform chemicals and perfumes (Alonso-Gutierrez et al., 2013), next generation biofuel compounds (Peralta-Yahya et al., 2011; Wang et al., 2011), cosmetics (McVean and Liebler, 1999), animal feed (Johnson et al., 1980), as well as food colorants (Baker and Günther, 2004).

Accepted manuscript

ACCEPTED MANUSCRIPT

As all organisms contain the metabolic precursors required to create terpenoid compounds, the capacity for heterologous overexpression of terpene synthases in industrially relevant microbial hosts has led to increasing interest in biotechnological production of these compounds (Kirby and Keasling, 2009). Heterologous over-production of terpenoid compounds in microbial systems can be superior to traditional extraction from natural sources due to containment and product yield consistency (Misawa, 2011). This strategy also minimizes the environmental impact of harvesting potentially rare organisms from their natural environment in order to acquire a desired terpenoid.

The most popular heterologous hosts for terpenoid production are bacteria and yeasts, as these organisms exhibit robust genetic tractability and can be cultured well at industrial scales. However, both rely on feeding with organic carbon sources such as glucose, cellulosic substrates, acetate, or methanol (Gruchattka and Kayser, 2015; Kirby and Keasling, 2009; Kirby et al., 2014). Although adaptable to current fermentation infrastructure, production relies on low cost of substrates which are subject to seasonal and market variability. As bio-industry shifts towards more sustainable processes, alternative hosts are required to match the goals of a carbon neutral bio-economy.

In contrast to fermentative systems, photosynthetic microbial hosts represent alternatives for many bio-production processes. Some photosynthetic hosts such as cyanobacteria and eukaryotic moss tissue culture have already been demonstrated to be amenable to heterologous terpenoid expression (Anterola et al., 2009; Davies et al., 2014; Halfmann et al., 2014; Zhan et al., 2014). Eukaryotic microalgae as photosynthetic production platforms, however, are notoriously difficult to genetically engineer and there are limited reports on synthetic metabolic modifications of these organisms (Cordero et al., 2011; Kaye et al., 2015). To date, no eukaryotic microalgal host has been used to demonstrate photosynthetically driven heterologous terpenoid production. Our goal in this study was to investigate the capacity of the model eukaryotic green microalga Chlamydomonas reinhardtii to produce heterologous sesquiterpenoids. Here, for the first time, we demonstrate robust overexpression of the patchoulol synthase from the plant Pogostemon cablin Benth (PcPs, (Deguerry et al., 2006)) in C. reinhardtii. We used the PcPs as a model terpene synthase to investigate the dynamics and possibilities of sesquiterpenoid production from the microalgal host. The PcPs was able to be overexpressed from codon optimized nuclear transgene constructs, the recombinant protein accumulated in the algal cytoplasm, and resulted in production of the sesquiterpenoid patchoulol from the native FPP pool. The capacity for precursor FPP enhancement through co-overexpression and fusions of the native FPPs, as well as bacterial and yeast FPPs were also

Accepted manuscript

ACCEPTED MANUSCRIPT

investigated. A novel strategy of gene loading via repetitive PcPs sequence fusions was demonstrated, resulting in multiple active sites per protein and the largest heterologous protein yet to be expressed in C. reinhardtii. Finally, we investigate cultivation parameters for photoautotrophic production of sesquiterpenoids from C. reinhardtii and compare production from this microalga with other photosynthetic microbial hosts.

2. Materials and Methods

2.1 C. reinhardtii strain

C. reinhardtii UVM4 cultures (graciously provided by Prof. Dr. Ralph Bock) were routinely maintained with TAP medium (Gorman and Levine, 1965) at 150 µmol photons m^{-2} s^{-1} light intensity in shake flasks or on TAP agar plates. UVM4 is an ultraviolet light derived mutant of CC-4350 (cw15 arg7-8 mt+ [Matagne 302]) which was co-transformed with the emetine resistance cassette CRY1 and ARG7, and demonstrated expression of nuclear transgenes with high efficiency (Neupert et al. 2009). CC-4350 is available from the Chlamydomonas Resource Center (http://chlamycollection.org).

2.2 Construct design, cloning, transformation, and mutant screening

All cloning in this work was performed with Fermentas Fastdigest restriction enzymes following manufacturer's protocols, alkaline phosphatase and ligation reactions were performed with the Rapid DNA Dephos & Ligation Kit (Roche). All PCRs were performed using Q5 High Fidelity polymerase with GC enhancer solution (New England Biolabs) following manufacturer's protocols with primers listed in Supplemental data file 1. After each cloning step, vector sequences were confirmed by sequencing (Sequencing Core Facility, CeBiTec, Bielefeld University, Germany).

The amino acid sequences for P. cablin patchoulol synthase (PcPs, UniProt: Q49SP3), Escherichia coli ispA (P22939), and Saccharomyces cerevisiae ERG20 (P08524) were codon optimized and synthesized (Genscript) as previously described (Lauersen et al., 2013). To each coding sequence the first intron (i1) of ribulose bisphosphate carboxylase small subunit 2 (RBCS2) was incorporated throughout the codon optimized sequences as this has been previously described to enhance transgene expression (Lumbreras et al., 1998). The synthetic nucleotide sequences for each construct can be accessed on the NCBI database: coPcPs (KX097887), coispA (KX097888), and coERG20 (KX097889). The genomic sequence for C. reinhardtii FPPs (A8IX41) was PCR amplified from genomic DNA and subjected to site directed mutagenesis to modify a single nucleotide to remove an NdeI site in the 5th intron.

Accepted manuscript

ACCEPTED MANUSCRIPT

Each sequence mentioned above was designed with compatible restriction endonuclease sites and cloned into pOpt_mVenus_Paro (NCBI:KM061060) or pOpt_mCerulean3_Hyg (KM061066) (Lauersen et al., 2015b), or amplified by PCR to create the fusion sequences described for vectors in Table 1. All constructs were oriented to create fusions with either mVenus (yellow) or mCerulean3 (cyan) fluorescent protein (Y/CFP) reporters.

Transformations were performed with glass bead agitation as previously described (Kindle, 1990). Positive transformants were recovered on TAP agar plates containing respective antibiotics at 10 mg L^{-1} with 200 µmol m^{-2} s^{-1} light intensity, and maintained on TAP agar plates with antibiotics by colony stamping. Antibiotic resistant colonies were then selected for target construct expression by either YFP or CFP fluorescence signal on the agar plate level as previously described (Lauersen et al., 2015b).

Colonies exhibiting fluorescence were picked to fresh plates, inoculated in 24-well clear microtitre plates with TAP medium and cultivated with 200 µmol m^{-2} s^{-1} light at 180 rpm until sufficiently dense. Cultures were then diluted in fresh medium to between $2x10^6$-$9x10^6$ cells mL^{-1}, fluorescence was measured in a TECAN plate reader and compared to cell count to determine the highest expressing strains. It was assumed that due to the position of the reporter proteins in the fusion, fluorescence expression indicated full-length construct expression. However, to ensure that outliers were not broken constructs expressing only the fluorescent reporter, mutants for each construct selected for biological triplicate product capture as described below were also subjected to SDS PAGE and Western blotting against the fluorescent reporter portion of the fusion protein (α-GFP, Life technologies) to confirm full-length construct expression.

Accepted manuscript

2.3 Fluorescence microscopy

7 µL of cells in TAP medium were mounted between a microscope slide and a high precision #1.5 coverglass (Marienfeld-Superior, Germany). The sample was sealed with nail polish and immediately imaged. Images were recorded on a Deltavision Elite microscope (GE Healthcare) with a 60x 1.42 N.A. oil immersion PlanApoN objective (Olympus Life Science) and an Evolve 512 EMCCD camera (Photometrics, Tucson AZ USA). The following excitation and emission wavelengths were used to record CFP, YFP, and chlorophyll signals: CFP excitation at 426-450 nm and emission at 463-487 nm, YFP excitation at 505-522 nm and emission at 537-559 nm, and chlorophyll excitation at 563-588 nm and emission at 603-648 nm. Several z planes were recorded at a distance of 250 nm. A single reference white-light differential interference contrast (DIC) image was also recorded. The fluorescent images were deconvolved

ACCEPTED MANUSCRIPT

with the appropriate recorded optical transfer function at default parameters for 10 iterations in the softWoRx 6.1.3 program (GE Healthcare). The background was averaged on deconvolved images with a gaussian blur at 1px width (Fiji/ImageJ package). The intensities were adjusted linearly: the background was subtracted with a value determined by the non-expressing controls for each channel, whereas the maximum intensities were individually adjusted for representation. The images shown represent a single deconvolution z-slice of a stack in the correct cell orientation.

2.4 Sesquiterpenoid capture and analysis

Screening of terpenoid productivity was conducted for each vector construct with three representative mutants each in biological triplicate. Cultivations were performed in 45 mL TAP medium containing shake flasks with 2.5 mL dodecane overlay. Cultivations were conducted with 200 µmol m^{-2} s^{-1} and 125 rpm shaking at 25 °C unless otherwise noted. After six days, cultures were harvested and dodecane was removed. Cell dry weight (CDW) was measured by centrifugation of either 5 or 10 mL of culture and incubation at 110 ˚C overnight. Dodecane fractions were recovered by pipette removal from the culture, followed by centrifugation at 20,000xg for 2 min. The clean dodecane fraction was then removed to new sample tubes and was used for gas chromatography-mass spectroscopy (GC-MS) analysis as described below. For carbon-use and scale-up investigations, cultivations were conducted in 380 mL media and 20 mL dodecane overlay. Cultures were stirred in 500 mL Schott bottles (9 cm diameter) with 400 µmol m^{-2} s^{-1} and either air or 3% CO_2 surface gassing. All cultivations were grown in biological triplicate with: TAP medium and air gassing, TAP medium with 2X regular phosphate concentration (TA2P) and air gassing, TA2P with 3% CO_2, as well as the same media lacking acetate (T2P) with 3% CO_2 gassing. TA2P and T2P media were set to pH 8.

The clean dodecane fractions were analyzed via GC-MS using a TraceGC gas chromatograph and ITQ ion trap mass spectrometer equipped with a AS 3000 autosampler (Thermo Scientific, Germany) and a 30-m x 0.25-mm VF-5 ms column coated with 0.25 µm of 5% diphenyl and 95% dimethylsiloxane (Varian GmbH, Darmstadt, Germany). Temperatures were set as follows, injector (250 °C), interface (250 °C) and ion source (220 °C). 1 µL of sample was injected in splitless mode. A constant flow of 1 mL min^{-1} helium was used as a carrier gas. The oven temperature was held at 80 °C for one minute, then raised to 120 °C at 10 °C min^{-1}, followed by 3 °C min^{-1} to 160 °C, and further to 270 °C at 10 °C min^{-1}, which was held for 2 min. Mass spectra were recorded after the dodecane peak eluted (12 min) using a scanning range of 50-750 m/z at 20 scans s^{-1}. Chromatograms were evaluated with Xcalibur software

Accepted manuscript

ACCEPTED MANUSCRIPT

version 2.0.7 (Thermo Scientific, Germany). The NIST 05 library (National Institute of Standards and Technology, Gaithersburg, MD; ThermoFinnigan) was used to identify substances, along with verification with a purified standard (PhytoLab GmbH, Vestenbergsgreuth, Germany). Standard calibration curves in the range of 1-450 µM patchoulol in dodecane were used to quantify the amount of patchoulol (peak lists and standard curve in Supplemental data file 2). 250 µM α-humulene was applied in each sample as internal standard. Extracted-ion chromatograms (XIC) with mass ranges of 91.00, 138.50, and 223.00 for samples with internal standard, and 138.00, 222.00 were used for samples without internal standards. All measurements were performed in triplicate and chromatograms were reviewed manually. Growth curves, peak lists and productivity data can be found in Supplemental data files 3-7 for all presented experiments.

2.5 Chlorophyll fluorescence measurements

The chlorophyll fluorescence parameters Fv/Fm and Φ_{PSII} were measured in a FluorCam FC 800-C instrument equipped with a high-resolution CCD camera (Photon System Instruments). Three 96-colony-plates (TAP_{Agar}) of parental strain UVM4 and the 3XPcPs mutant, respectively (n=288), were freshly prepared and cultivated at room temperature in the light for 69 h before chlorophyll fluorescence kinetics were determined. The measurements were performed by applying an adapted firmware Quenching Analysis protocol (Fluorcam7 v.1.0.12.0, illumination schedule: dark (5s) – saturating light (800ms) – dark (10s) – actinic light (180s) – dark (17s)). Values for Fo and Fm were determined before onset of the actinic light. Five additional saturating pulses were applied during the 180s actinic light exposure and Ft and Fm´ were determined at the end of this period. The chlorophyll fluorescence parameters Fv/Fm and Φ_{PSII} were calculated according to the equations Fv/Fm=(Fm-Fo)/Fm and Φ_{PSII}= (Fm´-Ft)/Fm´. Data can be found in Supplemental data 8.

3. Results and Discussion

3.1 Expression of the PcPs into the cytoplasm of C. reinhardtii results in patchoulol production.

Like many chlorophyte microalgae, C. reinhardtii contains only the 2-C-methyl-D-erythritol 4-phosphate (MEP) pathway for terpenoid biosynthesis (also known as 1-deoxy-D-xylulose 5-phosphate pathway (DOXP)), however, no melavonate (MVA) pathway as in higher plants and diatoms (Lohr et al., 2012). The terpenoid precursors found in the eukaryotic cell are produced

Accepted manuscript

ACCEPTED MANUSCRIPT

exclusively in the chloroplast and the mechanism of transport is not yet known (Fig. 1). Unlike the enzymes involved in the MEP pathway and synthesis of terpenoids related to photosynthesis, the FPP synthase from C. reinhardtii (A8IX41) lacks any detectible targeting peptides (analyzed with PredAlgo server). This suggested that if a free pool of the C15 sesquiterpene precursor FPP were to be found in the algal cell, it would be located in the cytoplasm. Therefore, nuclear based transgene expression was used to accumulate the PcPs as a cytoplasmic heterologous protein product.

It has been previously shown that some terpene synthases are capable of fusion to fluorescent reporters without effecting product generation (Albertsen et al., 2011). To increase the efficiency of identification of transformants with robust patchoulol synthase expression, the codon optimized PcPs gene was expressed in frame with YFP (mVenus) so that the fluorescent reporter was in fusion to the C-terminus of the patchoulol synthase. The PcPs was designed to contain a short and flexible GSG linker peptide on its C-terminus to minimize steric effects the fusion may have. YFP-fusion allowed colonies to be screened for fluorescence on primary transformant plates as previously described, owing to the robust nature of the fluorescent reporter (Lauersen et al., 2015b) (Fig. 2A). Initial transformants isolated as described above exhibited a distinct odour of patchoulol even on the agar plate level.

It was investigated whether two-phase cultivation with dodecane overlay would be appropriate for foreign sesquiterpenoid product capture from the cell wall-deficient C. reinhardtii UVM4 strain. Cultivation of the strain in 100 mL shake flasks with or without 5% dodecane overlay indicated that growth was indeed affected by solvent overlay, however, cultivation was possible with this two-phase system (Sup Fig. 1).

In order to determine the dynamics of patchoulol accumulation in dodecane, one mutant was selected and cultivated in TAP medium for eleven days with a dodecane overlay to capture patchoulol (Sup. Fig. 2A). Patchoulol was detected as a peak in GC-MS chromatograms of dodecane (Fig. 2B), and exhibited the appropriate mass fractionation pattern compared to the pure standard and database searches (Sup. Fig. 2B). This peak was not detected in the parental strain (Fig. 2B) or dodecane blanks. Our previous investigations of the dynamics of secreted recombinant proteins from C. reinhardtii had indicated that timing was essential to optimal product capture (Lauersen et al., 2015a). We were intrigued to observe that patchoulol accumulation increased in the dodecane fraction even after the cells had reached stationary phase (Sup. Fig. 2A). Accumulation occurred seemingly until catabolic processes ceased by 144 h, after which only minute accumulation occurred. Therefore, all further shake flask cultivations were harvested at 144 h to ensure total terpenoid capture.

Accepted manuscript

ACCEPTED MANUSCRIPT

Constructs were also designed which contained the PsaD or AtpA chloroplast or mitochondrial targeting peptides (Lauersen et al., 2015b; Rasala et al., 2014), respectively, in order to determine where subcellular pools of FPP may be within the cell (Sup. Fig. 3A). Although each construct expressed (Sup. Fig. 3B), no significant amounts of patchoulol were detected from mutants expressing either chloroplast or mitochondrial targeted PcPs-YFP (not shown). This suggested that the major pool of FPP is accessible in the cytoplasm, which is supported by the lack of predicted targeting peptides on the native C. reinhardtii FPPs.

Ten PcPs-YFP mutants with a range of construct expression were then chosen (normalized to cell density, depicted in Fig. 2A, black arrows). These strains were cultivated in triplicate 45 mL shake flasks with dodecane overlay. As expected, construct expression (fluorescence/cell) was correlated to higher performance in patchoulol yield in the dodecane layer (Fig. 2C). Fluorescence expression also correlated to relative protein abundance detected in Western blotting (Sup. Fig. 2C).

3.2 Sesquiterpene synthase titre, rather than FPP supply limits productivity

Although higher enzyme titres of the lone PcPs correlated to more product (Fig. 2C), no mutant was found with higher single PcPs expression than PcPs-YFP colony #18 which produced patchoulol up to 236 ± 14 µg g^{-1} CDW in 45 mL TAP shake flasks (Fig. 2C). It was unclear, however, if precursor FPP supply was limiting productivity, or whether enzyme titre was sufficient to exhaust the freely available FPP pool. Therefore, we chose PcPs-YFP #18 for co-overexpression studies with three different farnesyl diphosphate synthases: the lone native FPPs from C. reinhardtii, E. coli ispA, and S. cerevisiae ERG20. The codon-optimized sequences for each were cloned in fusion with the mCerulean3 (CFP) reporter in the pOpt_mCerulean3_Hyg vector (Lauersen et al., 2015b), which confers resistance to hygromycin B antibiotic (Fig. 3A). These constructs were transformed into PcPs-YFP #18 which was already paromomycin resistant. Colonies were then selected on plates containing both antibiotics, and positive transformants were screened for both YFP and CFP expression. Representative fluorescent cells are presented in Fig. 3B. Each construct expressed successfully, and signals were observed to exhibit appropriate molecular masses from both enzymes in total cellular protein samples by Western blotting (Sup. Fig. 4).

Three mutants generated with each vector, as well as three transformed with a CFP-only control, were selected and subsequently cultivated in triplicate shake flasks with dodecane overlay for patchoulol productivity. Although some individual mutants performed better in terms of patchoulol production (per g CDW, Fig. 3C), the second transformation round resulted

Accepted manuscript

ACCEPTED MANUSCRIPT

in isolation of transformants with variable PcPs-YFP levels, some much higher than that of the PcPs-YFP #18 strain. When patchoulol productivity from these strains was normalized to the fluorescence expression level of the PcPs construct (relative productivity (%), per pooled vector group) and compared to the three highest PcPs-YFP strains (colonies #5, 18, and 22, Fig. 2A), no co-expression strain outperformed the parental per CDW (Fig. 3C). These findings indicate that the PcPs enzyme titre, rather than the available FPP pool limited patchoulol production.

Surprisingly, the native FPPs of C. reinhardtii localized as a halo around the nucleus (Fig. 3B, CFP column, mutant with vectors iii+iv). This was not the case for either ispA or ERG20, which accumulated freely in the cytoplasm (Fig. 3B, CFP column, iii+v and iii+vi, respectively). The localization of CrFPPs is likely related to its role in sterol biosynthesis, as the endoplasmic reticulum surrounds the nucleus in this alga. However, there is no known mechanism responsible for such targeting, which may suggest that it has a strong binding partner with a downstream enzyme embedded in this region of the ER membrane. It is also unclear whether active transport or passive diffusion of IPP and DMAPP (or GPP and IPP) occurs to channel substrates to this location in the cell.

3.3 Precursor FPP synthase fusion to PcPs can increase patchoulol productivity

It has been previously demonstrated that fusion of the yeast ERG20 FPPs to a PcPs resulted in higher titers of patchoulol production in the yeast host, with the assumption that close proximity of FPP substrate generation to the PcPs active site increases substrate channelling to the synthase (Albertsen et al., 2011). Since high titers of the PcPs synthase were desired for robust productivity, and the CrFPPs exhibited specialized localization in the cell, only ispA and ERG20 were chosen for fusion trials with the PcPs. Both FPP synthases were cloned to create a fusion protein in frame with the N-terminus of the PcPs-YFP, resulting in constructs expressing ERG20-PcPs-YFP and ispA-PcPs-YFP fusion proteins (Fig. 4, vii and viii, respectively). These vectors were transformed and screened for expression by fluorescence as described above. Three mutants generated from each construct exhibiting fluorescence were cultivated in triplicate shake flasks and productivity analyzed by GC-MS of the dodecane overlay. Mutants identified by fluorescence containing the ERG20-PcPs-YFP fusion contained only partial protein constructs in Western blots (not shown) and also resulted in poor production of patchoulol (Fig. 4B, vii). The ispA-PcPs-YFP fusion, however, was expressed to full length (Sup. Fig. 5A), and resulted in a ~2.2 fold increase in relative productivity over constructs expressing the single PcPs in 45 mL TAP shake flasks (Fig. 4B, viii). It is unclear why it was

Accepted manuscript

ACCEPTED MANUSCRIPT

possible to express ERG20 as a fusion with CFP and not as a fusion to the PcPs-YFP as has been described in yeast (Albertsen et al., 2011), however, this was not investigated further in this work. The relative productivity of patchoulol normalized to enzyme expression was indeed higher for the strains expressing the ispA-PcPs fusion. It is, therefore, reasonable to propose that the proximity of FPP synthase can aid substrate channelling to the terpene synthase.

3.4 Increasing sesquiterpene synthase titre can increase relative product yield

Terpenoid synthase titre has previously been noted as a rate-limiting step in the production of monoterpenoids such as β-phellandrene (Formighieri and Melis, 2015). It was shown in this work that fusion of the β-phellandrene synthase to cpcB sequence, encoding for the abundant in cyanobacteria phycocyanin β-subunit, resulted in the fusion protein accumulating to ~20% total cellular protein in Synechocystis and increased β-phellandrene production 100-fold (Formighieri and Melis, 2015). It is unclear if such a strategy would work in C. reinhardtii, previously, a small subunit of Rubisco was fused to the mVenus reporter, and in this work the recombinant protein was only faintly detectible by Western blotting (Lauersen et al., 2015b). However, RBCS1 is part of the multi-subunit Rubisco complex and localized in the chloroplast. Future expression trials with the PcPs, could be conducted in fusion with abundant cytoplasmic proteins, such as actin or β-tubulin to determine whether a similar effect is possible in the eukaryotic host.

Transgene expression from the nuclear genome of C. reinhardtii generally results in low amounts of recombinant protein as a fraction of total protein (Barahimipour et al., 2015; Neupert et al., 2009). The maximum described in literature to date is 1% total soluble protein from a YFP in strain UVM11 (Barahimipour et al., 2015). Since it was determined here that the titre of terpene synthase was not yet sufficient to exhaust the freely available FPP pool within the cytoplasm of C. reinhardtii, we sought other methods to increase the titre of the PcPs. One strategy in over expression of target proteins is gene-loading, involving either high copy plasmids or multiple copies of a transgene expression cassette introduced into the genome (Aw and Polizzi, 2013). The only examples of multiple transgene expression from the nuclear genome of C. reinhardtii have been through double transformations with selectable markers (Lauersen et al., 2015b), mating of two separately expressing strains (Rasala et al., 2014), or using viral 2A peptides for cleavage (Rasala et al., 2014).

The PcPs sequence was also cloned to create a PcPs-CFP fusion in the hygromycin selection vector (Fig. 4A, ix). Double expression of the PcPs with both YFP and CFP fusions from two separate constructs was possible (Sup. Fig. 5B), and resulted in ~3 fold greater patchoulol

Accepted manuscript

ACCEPTED MANUSCRIPT

production normalized to YFP fluorescence, with one strain producing patchoulol up to 877 ± 153 µg g^{-1} CDW in 45 mL TAP shake flasks (Fig. 4B). It has been previously demonstrated that for YFP alone, multiple insertions of a transgene cassette into the genome did not result in higher expression titres (Barahimipour et al., 2015), however, by selecting for both reporters separately, mutants could be identified for robust expression of both YFP and CFP linked PcPs expression. The results indicate that increasing the amount of PcPs in the cell by double expression, PcPs-YFP + PcPs-CFP, increases relative patchoulol titres from the native FPP pool. This further suggested that enzyme titre, rather than substrate availability, was to this point the limiting factor of increasing sesquiterpene product yields.

Although co-overexpression of the PcPs-CFP in the PcPs-YFP #18 strain could increase total patchoulol yield, this required secondary transformation using hygromycin B resistance for selection and screening for the CFP reporter. This strategy limits the future engineering capabilities of this strain as it blocks further use of a valuable selection marker. Additionally, the second transformation round resulted in variable levels of the original PcPs-YFP construct, which has both positive and negative outcomes for productivity (see the individual mutants in Fig. 4B, iii+ix). Variable expression after secondary transformation for C. reinhardtii has been previously described (Lauersen et al., 2015b; Rasala et al., 2014). To circumvent these limitations, we next constructed repetitive fusions of the PcPs in two different orientations in vectors with paromomycin resistance: PcPs-YFP-PcPs and PcPs-PcPs-YFP (Fig. 4A, x and xi, respectively). These constructs allowed us to determine if two PcPs protein active sites could be expressed as one fusion protein, and whether the relative positions affected sesquiterpene production activities. Three transformants demonstrating fluorescence activity for each construct were selected and patchoulol productivity was determined as above. Each construct expressed as full-length protein, ~159 kDa (Sup. Fig. 5C). Relative to construct expression (fluorescence), both mutants performed as well as strains which had been double transformed with the PcPs-YFP + PcPs-CFP constructs in triplicate 45 mL TAP shake flasks (Fig. 4B).

A further vector was designed in which three PcPs sequences were fused in frame with the YFP on the C-terminus (Fig. 4A, xii). Interestingly, despite its large size and highly repetitive nature, this construct resulted in mutants which exhibited YFP fluorescence and also produced significant titres of patchoulol, up to 922 ± 242 µg g^{-1} CDW in 45 mL TAP shake flasks (Fig. 4B). Compared to the relative fluorescence, strains with the 3XPcPs-YFP construct produced ~4 fold more patchoulol over the single PcPs-YFP expressing strains normalized to CDW (Fig. 4B). This construct represents the largest heterologous protein expressed in C. reinhardtii to date with a confirmed apparent molecular mass of ~223.9 kDa (Sup. Fig. 5C).

Accepted manuscript

ACCEPTED MANUSCRIPT

Attempts were conducted to create a 4XPcPs-YFP fusion as well as a fusion of the ispA to constructs with 2X and 3XPcPs, however, no positive fluorescent clones could be identified which produced full-length protein products (Sup. Fig. 5C and not shown). To confirm that yields obtained from analysis of dodecane overlays were accurate, the 3XPcPs mutant was additionally cultivated in 45 mL flasks with and without dodecane. More patchoulol could be detected from cultures with dodecane overlay, than those without. Dodecane overlay resulted in ~99.5 % extraction from the system, with less than 0.5 % visible in pellets in both mid logarithmic and stationary phases (Sup. Fig. 5D).

The 3XPcPs mutant was then selected for further analysis in 100 mL TAP medium shake flask cultivations with or without dodecane overlay. 3XPcPs exhibited lower cell density than the parental strain UVM4, however, comparable CDW yields indicating larger cells for this mutant (Sup. Fig. 6). Chlorophyll fluorescence kinetics of UVM4 and the 3XPcPs mutant were analyzed to investigate if patchoulol production resulted in detrimental effects on the photosynthetic capacity of the cells. Replica plates of both strains (with a total of 288 colonies per strain) were investigated, but no indication for an altered photosystem II efficiency (Fv/Fm: UVM4 = 0.802 ± 0.001 (SEM); 3XPcPs = 0.807 ± 0.001 (SEM)) or detrimental effects on the linear electron flow (Φ_{PSII}: UVM4 = 0.42 ± 0.003 (SEM); 3XPcPs = 0.423 ± 0.002 (SEM)) were detectable in the mutant, indicating that these primary photosynthetic reactions were not negatively affected by the presence of patchoulol. It is likely that the production of patchoulol is in some way a stress to the cell, as cell size was larger compared to the parent, however, dodecane overlay did not relieve this effect as has been previously observed in cyanobacteria producing α-bisabolene (Davies et al., 2014).

3.5 Carbon source and sesquiterpene productivity in 400 mL batch cultivations

C. reinhardtii is able to be cultivated in several ways, photoautotrophically with light energy and CO_2 as a sole carbon source, on acetate, as well as combinations of these parameters (Sager and Granick, 1953). Acetate metabolism has allowed this organism to be used as a model for photosynthetic mutagenesis studies, since vital components of the photosynthetic apparatus can be knocked out, and the cells recovered heterotrophically (Rochaix, 1995). Here, mixotrophic acetate cultivations in TAP medium (light + acetate) allowed the high-throughput cultivation necessary to compare genetic constructs used for patchoulol production. However, the use of a microalga as a production host aims at leveraging its photosynthetic capacity for sustainable bio-production using light and CO_2 as inputs. Therefore, the effect of carbon source on sesquiterpenoid productivity was investigated with the 3XPcPs strain.

Accepted manuscript

ACCEPTED MANUSCRIPT

We wanted to directly compare CO_2, acetate, or acetate and CO_2 as carbon sources in the same medium to ensure differences were related only to carbon source. The most commonly used media for C. reinhardtii are Tris acetate phosphate (TAP), for acetate based growth, and high salt medium (HSM) for photoautotrophic cultivation (Gorman and Levine, 1965; Sueoka, 1960). However, our previous investigations of UVM4 indicated it was not possible to grow UVM4 in TP medium (TAP without acetate + 3% CO_2) due to pH shift issues (Lauersen et al., 2015a). Therefore, in order to have a medium in which direct comparisons of carbon sources could be made, several variations of TP medium were investigated and one containing 2X phosphate concentration at pH 8 was determined to promote the most stable cultivation of UVM4 (T2P is compared to HSM in Sup. Fig. 7). To standardize conditions, TAP with 2X phosphate at pH 8 (TA2P) and T2P media were used for carbon use comparisons of the 3XPcPs strain. Cultivations with TAP were also performed and the strain grew comparable to the modified media (not shown). Scale up in 400 mL volumes was conducted in T2P medium with 3 % CO_2, TA2P medium with air, and TA2P with CO_2 to compare: CO_2 alone, acetate alone, as well as CO_2+acetate, respectively (Fig. 5).

On each carbon source, growth proceeded as expected: CO_2 alone caused linear cell density and biomass increase over the 7 d cultivation, acetate resulted in stationary phase within 72 h, and the combination of both carbon sources boosted cell density and exhibited the highest biomass accumulation (Fig. 5A,B). Patchoulol was produced up to 351 ± 6 µg L^{-1} on CO_2 as a carbon source, 363 ± 41 µg L^{-1} on acetate, and 435 ± 25 µg L^{-1} with CO_2+acetate in 7 d (Fig. 5C). The PcPs is a promiscuous enzyme, and patchoulol accounts for only 34% of its sesquiterpene products from the C15 precursor FPP (Gruchattka and Kayser, 2015). It is therefore possible to estimate the total sesquiterpenoid yield from the system using patchoulol as a relative baseline, indicating a total sesquiterpenoid titer from the 3XPcPs strain of 1.03 mg L^{-1} in photoautotrophic conditions was achieved in 7 d of cultivation.

Interestingly, the yield of patchoulol relative to biomass was different depending on the carbon source provided (Fig. 5D). Patchoulol yield was 279 ± 15 µg g^{-1} CDW on CO_2, 520 ± 72 µg g^{-1} CDW on acetate, and 309 ± 14 µg g^{-1} CDW with both CO_2+acetate in 7 d.

The rates of production per volume for both cultivations with acetate exhibited peaks of productivity between 24-48 h, and steadily reduced throughout the cultivation (Fig. 5E). Photoautotrophic cultures, however, had a steadily increasing rate of production per volume throughout the cultivation (Fig. 5E). Rates of production relative to biomass were highest for all conditions between 24 and 48 h of cultivation in the early logarithmic phase, after which the production rates steadily decreased (Fig. 5F).

Accepted manuscript

ACCEPTED MANUSCRIPT

High productivity per biomass on acetate was achieved owing to the accumulation of patchoulol even after the cessation of culture growth by 72 h (Fig. 5A,B,C). This implies that intracellular metabolism was still occurring after acetate was exhausted from the medium, likely via breakdown of carbon storage compounds (starch), accumulated during the growth phase. Higher productivities on acetate may also be explained by consideration of the cellular metabolic processes that rely on FPP as a precursor. Unlike GPP and GGPP, FPP is not used for the production of terpenoids related to photosynthesis, rather, it is a precursor for sterols and ubiquinone (UQ). The latter is a key component in the mitochondrial electron transport chain (Fig. 1). C. reinhardtii lacks the MVA pathway, therefore, the FPP pool must be generated entirely from IPP and DMAPP produced in the chloroplast (Lohr et al., 2012). When acetate is fed to the cells, the main carbon metabolism is dependent on the ATP-requiring process of acetate uptake and conversion via the glyoxylate cycle into C4 components for cellular building blocks (Lauersen et al., 2016). Although ATP is generated by light and electron flow through photosystems in the chloroplasts, it is likely that the cells produce more FPP as a UQ precursor to drive aerobic respiration processes under ATP requiring, acetate consuming and low CO_2 conditions. In support of this argument, the CrFPPs (Cre03.g175250.t2.1) is strongly co-expressed with several subunits of the NADH ubiquinone oxidoreductase (17, 24, 10, 14, and 18 kDa subunits respectively, from Phytozome database C. reinhardtii v5.5). Indeed, the normalized production rates for acetate alone or mixed acetate and CO_2 cultivations were similar, supporting this observation (Fig. 5F). Here, both conditions exhibited similar patchoulol production rates within the first 48 h, when acetate was abundant, however, as acetate was consumed the rate decreased dramatically.

The results suggest that to increase the efficiency of photoautotrophic production of sesquiterpenes from the algal host, it will be necessary to modify the metabolism to boost FPP abundance as if acetate were the sole carbon source. Currently it is unclear if active transport or passive diffusion of IPP and DMAPP occurs from the chloroplast and whether this is the rate-liming step of FPP production, or whether it is controlled at the level of the CrFPPs. The FPKM (fragments per kilobase of exon per million fragments mapped) values for CrFPPs are similar for mixotrophic (18.292) and phototrophic (17.134) conditions (Phytozome v5.5 as above), indicating there is no transcriptional regulation of this enzyme between these two carbon modes. However, there is no known mechanism for active transport of IPP and DMAPP and no transporter for this process has been described. At this point, the source of metabolic push or pull driving the carbon flow in this pathway remains elusive. Determining the mechanism of regulation for FPP synthesis in C. reinhardtii will certainly be of great

Accepted manuscript

ACCEPTED MANUSCRIPT

importance to furthering the production potential of sesquiterpenoid products from this microalga.

3.6 Sesquiterpenoid productivity comparisons to other phototrophic microbial systems

There is growing interest in photosynthetic microbial bioproduction of many different products from light energy and CO_2. However, the majority of work done in this field has been with cyanobacterial strains, which are inherently more amenable to genetic engineering than eukaryotic microalgae. In addition to terpenoids, several other hydrocarbons have been produced via genetic engineering of photosynthetic cyanobacteria, for a recent review, the reader is directed to (Lai and Lan, 2015). Cyanobacterial systems have been used successfully to produce some hydrocarbons in the gram per litre range; ethanol to 5.50 g L^{-1} (Gao et al., 2012), isobutyraldehyde to 1.10 g L^{-1} (Atsumi et al., 2009), and 2,3-butanediol to 2.38 g L^{-1} (Oliver et al., 2013). However, heterologous terpenoid production from photosynthetic cyanobacteria have rarely been reported over a milligram per litre (Lai and Lan, 2015), with the sole exception of β-phellandrene production in Synechocystis described above in Section 3.4 (Formighieri and Melis, 2015). Three previous studies have used photosynthetic microbial systems specifically for sesquiterpenoid production: the moss Physcomitrella patens (Zhan et al., 2014), the cyanobacteria Synechococcus PCC 7002 (Davies et al., 2014), as well as Anabaena sp. PCC 7120 (Halfmann et al., 2014). Although P. patens is a eukaryotic plant, it is grown in liquid tissue culture in a similar way to microalgal cultivation. We therefore included it in this comparative analysis of photosynthetic microbial hosts.

Relative to biomass, P. patens expressing the PcPs alone was able to produce patchoulol up to 59 µg g CDW^{-1} d^{-1}, while The 3XPcPs mutant in our work was able to produce 40 µg g CDW^{-1} d^{-1} with CO_2 and 74 µg g CDW^{-1} d^{-1} on acetate (Table 2). Higher productivity of patchoulol relative to biomass was achieved after metabolic engineering for the moss, up to 96 µg g CDW^{-1} d^{-1}, when the truncated HMG-CoA reductase (tHMGR) of S. cerevisiae, the rate limiting step of the MVA pathway, was also expressed. Such a modification would not boost productivity for C. reinhardtii, because it lacks the MVA pathway (Lohr et al., 2012).

Volumetric productivities are also important when considering an expression platform, for the moss, no values of cell dry weight per volume were indicated in this publication, making direct comparison of volumetric productivities not possible. However, a similar study by the same research group recorded biomass of ~1 g CDW L^{-1} in 14 d for the moss cultivated under similar conditions (Pan et al., 2015). Assuming similar biomass, moss volumetric patchoulol productivities can be estimated to ~59 µg L^{-1} d^{-1} and ~81 µg L^{-1} d^{-1} for the PcPs alone and

ACCEPTED MANUSCRIPT

tHMGR-PcPs expression strains, respectively. In contrast, C. reinhardtii cultivation resulted in patchoulol productivity of ~50 μg L^{-1} d^{-1} with CO_2 and ~52 μg L^{-1} d^{-1} with acetate in 400 mL batch cultivations. The moss contains both the MEP and MVA pathways and should inherently have a greater pool of IPP and DMAPP channeled towards FPP production, likely explaining its higher overall productivities (Zhan et al., 2014). However, our analyses were conducted in 400 mL scale-up compared to shake flask cultivations of the moss. In shake flask screening on acetate, C. reinhardtii employing the 3XPcPs expression platform was able to achieve patchoulol productivities up to ~154 μg g CDW^{-1} d^{-1} relative to biomass and ~78 μg L^{-1} d^{-1} volumetrically, indicating that cultivation style may bias overall productivity between systems (Table 2).

Terpene synthases have different relative product profiles. For example patchoulol represents only ~34% of the sesquiterpene products made by the PcPs (Gruchattka and Kayser, 2015), while α–bisabolene and α–farnesene represent ~100% of the product profile from the Abies grandis (E)-α-bisabolene and Picea abies E,E-α-farnesene synthases, respectively (reviewed in (Degenhardt et al., 2009)). This allows comparisons of relative sesquiterpenoid production potential across hosts producing different sesquiterpenoids, although some variation in relative synthase reaction rates may affect overall yields in the same host. Both examples of cyanobacterial sesquiterpenoid engineering were conducted with terpene synthases that produce ~100% of their respective products as a single sesquiterpenoid. Therefore, comparison of yields from patchoulol producing strains requires estimation of total sesquiterpenoids produced from the PcPs by setting patchoulol as representative of ~34% of the total C15 products (Gruchattka and Kayser, 2015). Dodecane overlay for terpenoid product capture was also used for Synechococcus PCC 7002 expressing the AgBs, similar to that conducted in this work for C. reinhardtii, making this publication the most comparable to the eukaryotic microalga (Davies et al., 2014). The cyanobacterium produced α-bisabolene up to 75 μg g CDW^{-1} d^{-1}, with volumetric productivity of 150 μg L^{-1} d^{-1}. By comparison, estimation of total sesquiterpenoid production from C. reinhardtii with CO_2 as a carbon source was 117 μg g CDW^{-1} d^{-1}, and volumetric productivity of 147 μg L^{-1} d^{-1}. The results indicate that C. reinhardtii may have a higher native pool of freely available FPP for conversion to sesquiterpenes per gram dry biomass, or a greater potential per biomass to produce these products than the cyanobacteria. However, the cyanobacterium accumulated more biomass per unit time than the microalga, normalizing the relative volumetric production rates. However, total volumetric sesquiterpenoid productivity from C. reinhardtii was as high as 230 μg L^{-1} d^{-1} in 45 mL shake flask cultivations with acetate.

Accepted manuscript

ACCEPTED MANUSCRIPT

Anabaena sp. PCC 7120 was also shown to be able to produce α-farnesene, however, in this set-up a hydrophobic resin was used for head-space volatile product capture (Halfmann et al., 2014). No true values of culture biomass were given in this study, only optical density measurements, therefore, only volumetric productivities can be compared. In this set-up, Anabaena produced ~20 $\mu g\ L^{-1}\ d^{-1}$ total sesquiterpenoids (α-farnesene), well below that recorded for Synechococcus or C. reinhardtii. Clearly, cultivation style and product capture method have a strong impact on relative productivities for each system. Carbon source can also play a role in sesquiterpenoid productivity, as C. reinhardtii exhibited marked differences per biomass when the cells were cultivated on CO_2 or acetate. Our results suggest that the metabolic flexibility of C. reinhardtii may yet hold promise for significantly higher titers of photoautotrophic sesquiterpenoid production through metabolic engineering, if the factors responsible for this difference can be identified.

3.7 Conclusions

The pioneering work presented in this study has demonstrated the potential of the eukaryotic green microalga C. reinhardtii as a chassis for sesquiterpenoid production, and opened a new field of investigation for this valuable model organism. Our results indicate the cell has a relatively large, freely available, FPP pool which can be tapped to produce non-native metabolites. It is currently unknown what the upper limit of production from the native pool is in the algal host, and the routes forward for metabolic engineering targets are not apparently clear. However, it was determined here that a difference exists in FPP abundance within the alga dependent on carbon source, implying an inherent metabolic flexibility. Volumetrically, photoautotrophic cultivation could produce as much sesquiterpenoid product as acetate based growth, however, the relative rates of production demonstrated different dynamics. Determining the metabolic mechanisms of IPP and DMAPP transport, and the regulation of the FPP pool under different carbon regimes, will aid in the selection of metabolic engineering targets that could increase the flow of carbon precursors into desired products during photoautotrophic growth.

Accepted manuscript

Acknowledgements

The authors would like to acknowledge the Bielefeld Young Researchers' Fund (to KL), Cluster Industrial Biotechnology Graduate Cluster (CLIB-GC) (to TB), the European Union's Horizon 2020 grant agreement No 640720 Photofuel (to OK). The authors would like to

ACCEPTED MANUSCRIPT

express thanks to Prof. Dr. Ralph Bock for strain UVM4 and to Dr. Evamaria Gruchattka for her invaluable insights into this work.

Conflict of Interest

The authors declare that they have no conflict of interest.

References

Albertsen, L., Chen, Y., Bach, L.S., Rattleff, S., Maury, J., Brix, S., Nielsen, J., Mortensen, U.H., 2011. Diversion of flux toward sesquiterpene production in Saccharomyces cerevisiae by fusion of host and heterologous enzymes. Appl Environ Microbiol 77, 1033–40. doi:10.1128/AEM.01361-10

Alonso-Gutierrez, J., Chan, R., Batth, T.S., Adams, P.D., Keasling, J.D., Petzold, C.J., Lee, T.S., 2013. Metabolic engineering of Escherichia coli for limonene and perillyl alcohol production. Metab Eng 19, 33–41. doi:10.1016/j.ymben.2013.05.004

Anterola, A., Shanle, E., Perroud, P.-F., Quatrano, R., 2009. Production of taxa-4(5),11(12)-diene by transgenic Physcomitrella patens. Transgenic Res 18, 655–60. doi:10.1007/s11248-009-9252-5

Atsumi, S., Higashide, W., Liao, J.C., 2009. Direct photosynthetic recycling of carbon dioxide to isobutyraldehyde. Nat Biotechnol 27, 1177–80. doi:10.1038/nbt.1586

Aw, R., Polizzi, K.M., 2013. Can too many copies spoil the broth? Microb Cell Fact 12, 128. doi:10.1186/1475-2859-12-128

Baker, R., Günther, C., 2004. The role of carotenoids in consumer choice and the likely benefits from their inclusion into products for human consumption. Trends Food Sci Technol 15, 484–488. doi:10.1016/j.tifs.2004.04.0094

Barahimipour, R., Strenkert, D., Neupert, J., Schroda, M., Merchant, S.S., Bock, R., 2015. Dissecting the contributions of GC content and codon usage to gene expression in the model alga Chlamydomonas reinhardtii. Plant J n/a–n/a. doi:10.1111/tpj.13033

Beekwilder, J., van Houwelingen, A., Cankar, K., van Dijk, A.D.J., de Jong, R.M., Stoopen, G., Bouwmeester, H., Achkar, J., Sonke, T., Bosch, D., 2014. Valencene synthase from the heartwood of Nootka cypress (Callitropsis nootkatensis) for biotechnological production of valencene. Plant Biotechnol J 12, 174–182. doi:10.1111/pbi.12124

Buckingham, J., Macdonald, F.M., Bradley, H.M., Cai, Y., Munasinghe, V.R.N., Pattenden, C.F., 1994. Dictionary of natural products, 1st ed. Chapman and Hall, London.

Cordero, B.F., Couso, I., León, R., Rodríguez, H., Vargas, M.A., 2011. Enhancement of carotenoids biosynthesis in Chlamydomonas reinhardtii by nuclear transformation using a phytoene synthase gene isolated from Chlorella zofingiensis. Appl Microbiol Biotechnol 91, 341–51. doi:10.1007/s00253-011-3262-y

Davies, F.K., Work, V.H., Beliaev, A.S., Posewitz, M.C., 2014. Engineering Limonene and Bisabolene Production in Wild Type and a Glycogen-Deficient Mutant of Synechococcus sp. PCC 7002. Front Bioeng Biotechnol 2, 21. doi:10.3389/fbioe.2014.00021

Degenhardt, J., Köllner, T.G., Gershenzon, J., 2009. Monoterpene and sesquiterpene synthases and the origin of terpene skeletal diversity in plants. Phytochemistry 70, 1621–37. doi:10.1016/j.phytochem.2009.07.030

Deguerry, F., Pastore, L., Wu, S., Clark, A., Chappell, J., Schalk, M., 2006. The diverse sesquiterpene profile of patchouli, Pogostemon cablin, is correlated with a limited number of sesquiterpene synthases. Arch Biochem Biophys 454, 123–136. doi:10.1016/j.abb.2006.08.006

Formighieri, C., Melis, A., 2015. A phycocyanin·phellandrene synthase fusion enhances

Accepted manuscript

ACCEPTED MANUSCRIPT

recombinant protein expression and β-phellandrene (monoterpene) hydrocarbons production in Synechocystis (cyanobacteria). Metab Eng 32, 116–124. doi:10.1016/j.ymben.2015.09.010

Gao, Z., Zhao, H., Li, Z., Tan, X., Lu, X., 2012. Photosynthetic production of ethanol from carbon dioxide in genetically engineered cyanobacteria. Energy Environ Sci 5, 9857–9865. doi:10.1039/C2EE22675H

Gershenzon, J., Dudareva, N., 2007. The function of terpene natural products in the natural world. Nat Chem Biol 3, 408–14. doi:10.1038/nchembio.2007.5

Gorman, D.S., Levine, R.P., 1965. Cytochrome f and plastocyanin: their sequence in the photosynthetic electron transport chain of Chlamydomonas reinhardi. Proc Natl Acad Sci 54, 1665–1669. doi:10.1073/pnas.54.6.1665

Gruchattka, E., Kayser, O., 2015. In Vivo Validation of In Silico Predicted Metabolic Engineering Strategies in Yeast: Disruption of α-Ketoglutarate Dehydrogenase and Expression of ATP-Citrate Lyase for Terpenoid Production. PLoS One 10, e0144981. doi:10.1371/journal.pone.0144981

Halfmann, C., Gu, L., Gibbons, W., Zhou, R., 2014. Genetically engineering cyanobacteria to convert CO2, water, and light into the long-chain hydrocarbon farnesene. Appl Microbiol Biotechnol 98, 9869–9877. doi:10.1007/s00253-014-6118-4

Johnson, E.A., Villa, T.G., Lewis, M.J., 1980. Phaffia rhodozyma as an astaxanthin source in salmonid diets. Aquaculture 20, 123–134. doi:doi:10.1016/0044-8486(80)90041-1

Kaye, Y., Grundman, O., Leu, S., Zarka, A., Zorin, B., Didi-Cohen, S., Khozin-Goldberg, I., Boussiba, S., 2015. Metabolic engineering toward enhanced LC-PUFA biosynthesis in Nannochloropsis oceanica: Overexpression of endogenous Δ12 desaturase driven by stress-inducible promoter leads to enhanced deposition of polyunsaturated fatty acids in TAG. Algal Res. doi:10.1016/j.algal.2015.05.003

Kindle, K.L., 1990. High-frequency nuclear transformation of Chlamydomonas reinhardtii. Proc Natl Acad Sci USA 87, 1228–1232.

Kirby, J., Keasling, J.D., 2009. Biosynthesis of plant isoprenoids: perspectives for microbial engineering. Annu Rev Plant Biol 60, 335–55. doi:10.1146/annurev.arplant.043008.091955

Kirby, J., Nishimoto, M., Chow, R.W.N., Baidoo, E.E.K., Wang, G., Martin, J., Schackwitz, W., Chan, R., Fortman, J.L., Keasling, J.D., 2014. Enhancing Terpene Yield from Sugars via Novel Routes to 1-Deoxy-D-Xylulose 5-Phosphate. Appl Environ Microbiol 81, 130–138. doi:10.1128/AEM.02920-14

Lai, M., Lan, E., 2015. Advances in Metabolic Engineering of Cyanobacteria for Photosynthetic Biochemical Production. Metabolites 5, 636–658. doi:10.3390/metabo5040636

Lange, B.M., Rujan, T., Martin, W., Croteau, R., 2000. Isoprenoid biosynthesis: The evolution of two ancient and distinct pathways across genomes. Proc Natl Acad Sci 97, 13172–13177. doi:10.1073/pnas.240454797

Lauersen, K.J., Berger, H., Mussgnug, J.H., Kruse, O., 2013. Efficient recombinant protein production and secretion from nuclear transgenes in Chlamydomonas reinhardtii. J Biotechnol 167, 101–110. doi:http://dx.doi.org/10.1016/j.jbiotec.2012.10.010

Lauersen, K.J., Huber, I., Wichmann, J., Baier, T., Leiter, A., Gaukel, V., Kartushin, V., Rattenholl, A., Steinweg, C., von Riesen, L., Posten, C., Gudermann, F., Lütkemeyer, D., Mussgnug, J.H., Kruse, O., 2015a. Investigating the dynamics of recombinant protein secretion from a microalgal host. J Biotechnol 215, 62–71. doi:10.1016/j.jbiotec.2015.05.001

Lauersen, K.J., Kruse, O., Mussgnug, J.H., 2015b. Targeted expression of nuclear transgenes in Chlamydomonas reinhardtii with a versatile, modular vector toolkit. Appl Microbiol

Accepted manuscript

Biotechnol 99, 3491–3503. doi:10.1007/s00253-014-6354-7

Lauersen, K.J., Willamme, R., Coosemans, N., Joris, M., Kruse, O., Remacle, C., 2016. Peroxisomal microbodies are at the crossroads of acetate assimilation in the green microalga Chlamydomonas reinhardtii. Algal Res 16, 266–274. doi:10.1016/j.algal.2016.03.026

Lohr, M., Schwender, J., Polle, J.E.W., 2012. Isoprenoid biosynthesis in eukaryotic phototrophs: A spotlight on algae. Plant Sci. doi:10.1016/j.plantsci.2011.07.018

Lumbreras, V., Stevens R., D., Purton, S., 1998. Efficient foreign gene expression in Chlamydomonas reinhardtii mediated by an endogenous intron. Plant J 14, 441–447.

McVean, M., Liebler, D.C., 1999. Prevention of DNA photodamage by vitamin E compounds and sunscreens: roles of ultraviolet absorbance and cellular uptake. Mol Carcinog 24, 169–176.

Misawa, N., 2011. Pathway engineering for functional isoprenoids. Curr Opin Biotechnol 22, 627–33. doi:10.1016/j.copbio.2011.01.002

Neupert, J., Karcher, D., Bock, R., 2009. Generation of Chlamydomonas strains that efficiently express nuclear transgenes. Plant J 57, 1140–1150. doi:10.1111/j.1365-313X.2008.03746.x

Nosten, F., White, N.J., 2007. Artemisinin-based combination treatment of falciparum malaria. Am J Trop Med Hyg 77, 181–92.

Oliver, J.W.K., Machado, I.M.P., Yoneda, H., Atsumi, S., 2013. Cyanobacterial conversion of carbon dioxide to 2,3-butanediol. Proc Natl Acad Sci U S A 110, 1249–54. doi:10.1073/pnas.1213024110

Pan, X.W., Han, L., Zhang, Y.H., Chen, D.F., Simonsen, H.T., 2015. Sclareol production in the moss Physcomitrella patens and observations on growth and terpenoid biosynthesis. Plant Biotechnol Rep 9, 149–159. doi:10.1007/s11816-015-0353-8

Pateraki, I., Heskes, A.M., Hamberger, B., 2015. Cytochromes P450 for Terpene Functionalisation and Metabolic Engineering, in: Advances in Biochemical Engineering/biotechnology. pp. 107–139. doi:10.1007/10_2014_301

Peralta-Yahya, P.P., Ouellet, M., Chan, R., Mukhopadhyay, A., Keasling, J.D., Lee, T.S., 2011. Identification and microbial production of a terpene-based advanced biofuel. Nat Commun 2, 483. doi:10.1038/ncomms1494

Rasala, B.A., Chao, S.-S., Pier, M., Barrera, D.J., Mayfield, S.P., 2014. Enhanced genetic tools for engineering multigene traits into green algae. PLoS One 9, e94028. doi:10.1371/journal.pone.0094028

Rochaix, J.D., 1995. Chlamydomonas reinhardtii as the photosynthetic yeast. Annu Rev Genet 29, 209–230. doi:10.1146/annurev.ge.29.120195.001233

Sager, R., Granick, S., 1953. Nutritional studies with Chlamydomonas reinhardi. Ann N Y Acad Sci 56, 831–838. doi:10.1111/j.1749-6632.1953.tb30261.x

Sueoka, N., 1960. Mitotic replication of deoxyribonucleic acid in Chlamydomonas reinhardii. Proc Natl Acad Sci 46, 83–91.

Wang, C., Yoon, S.-H., Jang, H.-J., Chung, Y.-R., Kim, J.-Y., Choi, E.-S., Kim, S.-W., 2011. Metabolic engineering of Escherichia coli for α-farnesene production. Metab Eng 13, 648–655. doi:10.1016/j.ymben.2011.08.001

Weitzel, C., Simonsen, H.T., 2013. Cytochrome P450-enzymes involved in the biosynthesis of mono- and sesquiterpenes. Phytochem Rev 1–18. doi:10.1007/s11101-013-9280-x

Zhan, X., Zhang, Y., Chen, D., Simonsen, H.T., 2014. Metabolic engineering of the moss Physcomitrella patens to produce the sesquiterpenoids patchoulol and -santalene. Front Plant Sci 5. doi:10.3389/fpls.2014.00636

Accepted Manuscript

ACCEPTED MANUSCRIPT

Fig 1 Upper panel: lateral slice diagram of the unicellular green algae C. reinhardtii. Flagella are shown with a dotted line indicating their conditional absence. Major cellular compartments are indicated: **M** mitochondria, depicted here as independent, however form a reticular network around the chloroplast, **N** nucleus, **ER** endoplasmic reticulum, **m** peroxisomal microbodies, **C** chloroplast. The two major cellular carbon sinks are starch, found in the pyrenoid (**P**) and triacylglycerols in lipid droplets (**L**). Lower panel: overview of terpenoid metabolism in C. reinhardtii, the 2-C-methyl-D-erythritol 4-phosphate (MEP) pathway is found in the chloroplast made up of imported nuclear encoded proteins (abbreviated in blue). Farnesyl diphosphate synthase (**FPPs**) is not located in the chloroplast, and its C15 product, FPP, is used in other cellular compartments for native terpenoid compounds. The overexpression of a terpene synthase in the cytoplasm diverts freely available FPP for sesquiterpenoid production, the chemical structure of patchoulol is depicted. Abbreviations: **DXS** 1-deoxy-D-xylulose 5-phosphate synthase (Uniprot: O81954), product: 1-deoxy-D-xylulose 5-phosphate (DXP). **DXR** 1-deoxy-D-xylulose 5-phosphate reductoisomerase (A8IY85), product: 2-C-methyl-D-erythriol 4-phosphate (MEP). **MCT** 2-C-methyl-D-erythritol 4-phosphate cytidylyltransferase (A8JAC5 alternative name for C. reinhardtii: CMS), product: 4-diphosphocytidyl-2-C-methylerythritol (CDP-ME). **CMK** 4-(cytidine 5'-diphospho)-2-C-methyl-D-erythritol kinase (A8J0V1), product: 4-diphosphocytidyl-2-C-methyl-D-erythritol 2-phosphate (CDP-MEP). **MDS** 2-C-methyl-D-erythritol 2,4-cyclodiphosphate synthase (A8IJL3 alternative name: MEC), product: 2-C-methyl-D-erythritol 2,4-cyclodiphosphate (MEcPP). **HDS** 4-hydroxy-3-methylbut-2-en-1-yl diphosphate synthase (A8ILN4), product: (E)-4-Hydroxy-3-methyl-but-2-enyl diphosphate (HMB-PP). **HDR** 4-hydroxy-3-methylbut-2-en-1-yl diphosphate reductase (A8JEV9 alternative name: IDS), products: IPP and DMAPP. **IDI** isopentenyl diphosphate:dimethylallyl diphosphate isomerase (A8JF38). **GPPs?** geranyl diphosphate synthase (A8IKV5, PredAlgo targeting prediction of this protein is to the mitochondria, therefore a ? is included, function and targeting in C. reinhardtii is not currently clear), proposed product: geranyl diphosphate (C10). **GGPPs** geranylgeranyl diphosphate synthase (A8JHU6), product: geranylgeranyl diphosphate (C20). **GGR** geranylgeranyl reductase (A8HNE8). **FPPs** farnesyl diphosphate synthase (A8IX41), product: farnesyl diphosphate (C15). **SPPs** solanesyl diphosphate synthase (A8HRQ4), product: solanesyl diphosphate (C45). **PPPs** polyprenyl diphosphate synthase (A8HX47, Phytozome v5.5, termed FPP specific PPs). **PSY** phytoene synthase (Q6J214). **T?** it is unknown if transporters are responsible for IPP and DMAPP export from the chloroplast and FPP import to the mitochondria.

Accepted manuscript

ACCEPTED MANUSCRIPT

Fig 2 Overview of expression and screening strategy for the patchoulol synthase and other constructs in this work. **A** Diagram of the codon optimized patchoulol synthase in fusion with the mVenus reporter in the pOpt_mVenus_Paro vector. Blue rectangles in the vector diagram indicate the RBCS2(i1) intron copies spread throughout the codon optimized sequence, the codon optimized mVenus and mCerulean3 reporters were previously described to contain the RBCS2(i2) intron. All constructs in this work were transformed into C. reinhardtii strains and recovered on selective antibiotic conditions as depicted. The fluorescent protein fusions allowed direct screening for expressing strains on the agar plate level which were then isolated, and cultivated in microtitre plates where fluorescence expression per cell was determined. This screening method allowed straightforward identification of mutants expressing high levels of the target-fluorescent protein fusions. Black arrows represent ten mutants with variable expression levels which were tested for patchoulol productivity with dodecane overlay in shake flasks. **B** Patchoulol (retention time of 19.8 min) could be detected readily by GC-MS in dodecane samples used as two-phase overlay in shake flasks. α-humulene is shown as an internal standard (~14 min), the presented chromatograms are from individual colonies depicted for fluorescence as numbered in the bar graph above (col. 18 and 23), no peak for patchoulol was detectible in dodecane samples from the parental strain (WT). **C** Relative productivity in two-phase dodecane overlay screening of mutants correlated with the original fluorescence expression per cell identified in screening, colonies 18 and 23 are indicated. Error bars represent 95% confidence interval.

Fig 3 Attempts to boost precursor pool by FPP synthase overexpression in patchoulol producing strains. **A** Vectors for expression of fluorescent reporters YFP and CFP (i and ii, respectively), the codon optimized P. cablin patchoulol synthase (PcPs) (iii), the native FPP synthase of C. reinhardtii (iv), as well as the codon optimized FPP synthases of E. coli (ispA, v) and S. cerevisiae (ERG20, vi). The respective selection markers are indicated for paromomycin (Paro) or hygromycin B (Hyg) from the respective pOptimized vectors described in the Material and Methods. The CrFPPs contains 11 natural introns. **B** Fluorescence microscopy images of individual representatives identified in screening. The signals obtained for respective filters are indicated. WT – parental strain UVM4. Scale bars represent 5 µm. The vectors used are indicated to the right of each image. For constructs with two vectors, the paromomycin resistance vector was transformed first and a mutant with robust expression for that construct identified which was then subjected to transformation and screening of constructs containing the hygromycin B selection marker. **C** Three mutants identified from each pool of transformants were cultivated in triplicate with two-phase dodecane overlay and compared for

Accepted manuscript

ACCEPTED MANUSCRIPT

patchoulol productivities (left). The relative productivity (right) was determined by normalizing the obtained patchoulol productivity to the fluorescence expression determined of each strain. Yellow bars indicate a strain expressing a YFP linked expression construct only, while yellow-cyan gradients represent mutants expressing both YFP and CFP- linked constructs from separate vectors as described above. Data obtained from mutants expressing the single PcPs expression vector (iii) was set as 100%. Error bars represent 95% confidence interval.

Fig 4 PcPs fusion vectors and their respective patchoulol productivities. **A** Vector diagrams of the expression cassettes built into the pOptimized vectors. The codon optimized sequences of ERG20 and ispA were cloned in frame to form fusion proteins with the PcPs-YFP (vii and viii, respectively). The PcPs was cloned into the pOpt_mCerulean3_Hyg vector to allow double transformation with a second selection marker and reporter (ix). Double (x and xi) and triple (xii) copies of the PcPs were cloned into the pOpt_mVenus_Paro vector in order to determine whether multiple active sites could be expressed as a large protein fusion from a single genetic construct to achieve synthetic gene loading. **B** Three mutants derived from transformation with each construct were cultivated in triplicate with two-phase dodecane overlay and compared for relative patchoulol productivities (left). The relative productivity (right) was determined by normalizing the obtained patchoulol productivity to the fluorescence expression determined of each strain. The yellow-cyan gradient represents mutants expressing both YFP and CFP- linked PcPs constructs from separate vectors as described above. Data obtained from mutants expressing the single PcPs expression vector (iii) was set as 100%. Error bars represent 95% confidence interval.

Fig 5 3XPcPs expression strain growth and patchoulol productivity in 400 mL batch cultivations with different carbon sources. Cultures were grown in biological triplicate in modified media with a 5% dodecane overlay as described in the Material and Methods. Acetate, 3% CO_2, or acetate and CO_2 were supplied as carbon sources for cell growth. Cell density (**A**) and cell dry weight (**B**) were recorded daily, in addition patchoulol productivity was measured daily from the dodecane overlay by GC-MS (**C**). Daily sampling permitted the determination of patchoulol yield per dry weight (**D**) and per cell (**E**) from each carbon source. From these values, the relative patchoulol production rates could be calculated for each day of cultivation (**F**). Error bars represent 95% confidence interval.

Supplemental Figure 1 Dodecane overlay effects on cell wall deficient C. reinhardtii culture growth. Cell density and cellular dry weight are shown for C. reinhardtii strain UVM4

Accepted manuscript

ACCEPTED MANUSCRIPT

cultivated in shake flasks with 100 mL TAP medium with or without 5% dodecane overlay. Error bars represent 95% confidence interval.

Supplemental Figure 2 Patchoulol captured in dodecane accumulates throughout cultivation. **A** PcPs expressing strain cultivated for 11 days demonstrates patchoulol accumulation in dodecane overlay past the stationary phase of cell growth. Error bars represent 95% confidence interval. **B** Mass fractionation of peaks identified in GC-MS of dodecane samples from PcPs expression strains (upper panel) match that obtained from pure patchoulol standard (lower panel). **C** Ten separate PcPs-YFP expressing mutants (numbers correspond to black arrows in Figure 1A) demonstrate single PcPs-YFP protein product at the appropriate predicted molecular mass (~94.3 kDa) after total cellular proteins were run on 8% SDS PAGE gels and subjected to Western blotting with an α-GFP antibody. The parental strain (P) and strain expressing the mVenus (YFP) reporter alone (Y) are shown as controls. Ponceau S stain is shown on the nitrocellulose membrane as a loading control. M - PageRuler™ Plus Prestained Protein Ladder (Thermofisher Scientific).

Supplemental Figure 3 Vector constructs for organelle targeting of the PcPs-YFP fusion. **A** diagrams of the mitochondrial (AtpA, iii^{m}) and chloroplast (PsaD, iii^{c}) targeted PcPs-YFP expression vectors are shown with PcPs-YFP (iii) and pOpt_mVenus_Paro (i) controls. **B** Representative fluorescence microscopy images of strains identified to have fluorescent signals after transformation with each respective vector. WT - parental strain UVM4. Scale bars represent 5 µm.

Supplemental Figure 4 8% SDS PAGE and Western blot of the triplicate strains used to generate data for Figure 3. M – marker, P – parental strain UVM4. Sample 1: PcPs-YFP colony #18 from Figure 2, the single protein product is visible at ~94.3 kDa for this and all subsequent strains. Samples 2-4: PcPs-YFP #18 transformed with CrFPPs-CFP-Hyg vector, the CrFPPs-CFP fusion can be seen as a band at ~70.3 kDa. Samples 5-7: PcPs-YFP colony #18 transformed with ispA-CFP-Hyg vector, the fusion product can be seen a band at ~62.2 kDa. Samples 8-10: PcPs-YFP colony #18 transformed with ERG20-CFP hygro expression vector, the ERG20-CFP product is detectable as a band at ~70.8 kDa. Samples 11-13: PcPs-YFP colony #18 transformed with pOpt_mCerulean3_Hyg control vector, the CFP product is 30.2 kDa and was below the running front of this gel, however, clearly detected in fluorescence microscopy (Figure 3). The α-GFP antibody binds to both mVenus (YFP) and mCerulean3 (CFP) protein products, allowing detection of the fusion protein products by Western blot. Ponceau S stain is shown on the nitrocellulose membrane as a loading control.

Accepted manuscript

ACCEPTED MANUSCRIPT

Supplemental Figure 5 Confirmation of protein product size for gene expression constructs depicted in Figure 4. **A** M – marker, P – parental strain UVM4. Sample 1: PcPs-YFP colony #18 from Figure 2, the single protein product is visible at ~94.3 kDa. Individual mutants expressing the ispA-PcPs-YFP fusion (samples 2-4, vector viii) exhibit a band detectible with an apparent molecular mass of ~127.5 kDa. **B** The PcPs-YFP and PcPs-CFP protein products overlap with the same apparent molecular mass on Western blots, therefore, a fluorescence image is shown for CFP and YFP expression in strains generated by transformation of both vectors iii and ix. The images were recorded with the same settings used in Figure 3, the scale bar represents 5 µm. **C** M – marker, P – parental strain UVM4. Sample 1: PcPs-YFP colony #18 from Figure 2, the single protein product is visible at ~94.3 kDa. Samples: 2-4 a band at the apparent molecular mass of ~159.2 kDa is visible in strains expressing PcPs-YFP-PcPs (vector x). Samples: 5-7 a band at the apparent molecular mass of ~159.4 kDa is visible in strains expressing PcPs-PcPs-YFP (vector xi). Samples: 8-10 a band at the apparent molecular mass of ~223.9 kDa is visible in strains expressing PcPs-PcPs-PcPs-YFP (vector xii), sample 10 had very low expression, and no band could be confirmed for this strain, although relative productivity was appropriate for full length construct expression (Figure 4). Samples 11-13 were generated with a vector expressing four copies of the PcPs, however, no full length protein product could be confirmed. Total cellular proteins were run on 8% SDS PAGE gels and subjected in Western blotting with an α-GFP antibody. Ponceau S stain is shown on the nitrocellulose membrane as a loading control. **D** Fraction of patchoulol partitioned into dodecane. Cells with or without dodecane overlay were harvested at 72 and 120 h, dodecane samples were measured directly, while cell pellets and culture supernatant were subjected to dodecane extraction by vortexing. With dodecane overlay, more total patchoulol could be detected in the system and only 0.5% of detectible patchoulol was found left in the cell pellet of cultures. Patchoulol could be detected in both the cell pellet and culture supernatant in cultures without overlay, where the product was split between both phases.

Supplemental Figure 6 Growth curve analysis comparison of UVM4 and the 3XPcPs expression strain with and without dodecane overlay in shake flasks. Cell density and dry biomass were recorded daily for these strains. Values for UVM4 cultivation are taken from Supplemental Figure 1, however, the cultivation experiment was conducted at the same time. Error bars represent 95% confidence interval.

Supplemental Figure 7 Comparison of HSM and T2P media for photoautotrophic cultivation of UVM4. Cell density and dry biomass were measured daily in 400 mL stirred cultivations with 3% CO_2 surface gassing. T2P media is derived from TAP media without acetate and 2X

Accepted manuscript

ACCEPTED MANUSCRIPT

phosphate concentrations. It was determined to be the most stable condition to grow strain UVM4 for direct carbon-source comparative studies in this work. Error bars represent 95% confidence interval.

Supplemental data file captions

Supplemental data file 1 - Primers used in this study A list of cloning primers used for vector constructs as listed in Table 1.

Supplemental data 2 - Patchoulol standard quantification and peak lists individual peak lists and calculations for patchoulol standard quantification.

Supplemental data 3 - 11 day culture growth and peak lists Sup Fig. 2A data used to create Sup. Fig. 2A.

Supplemental data 4 - Growth and productivity for 1xPcPs - 10 mutants in Figure 2 Data used to create Figure 2.

Supplemental data 5 - GCMS Peak lists Figures 2,3,4 GC-MS data used to create Figures 2, 3, and 4.

Supplemental data 6 - Patchoulol productivity data Figures 2,3,4 Growth data and calculations used for patchoulol productivity in Figures 2, 3, and 4.

Supplemental data 7 - 400 mL cultivation productivity and peak lists Figure 5 cultivation and GCMS peak list data used for Figure 5.

Supplemental data 8 - photosynthetic comparisons of UVM4 and 3XPcPs fluorescence data used to determine photosynthetic capacity of UVM4 and 3XPcPs

Table 1: Genetic constructs used in this study

Construct name	Vector	Antibiotic resistance in C. reinhardtii	Gene length with introns from start codon to stop (bp)	CDS (bp)	RBCS2 i1 copies	Protein length (aa)	Predicted molecular weight (kDA)	Accession No. (NCBI)
pOpt_mVenus_Paro	**i**	paromomycin	1281	807	1	268	30.4	KM061060
pOpt_mCerulean3_Hyg	**ii**	hygromycin B	1281	807	1	268	30.2	KM061066
PcPs_YFP	**iii**	paromomycin	3384	2475	4	824	94.3	cloned in v:**i**
CrFPPs_CFP	**iv**	hygromycin B	4827	1878	1*	625	70.3	v:**ii**

Accepted manuscript

ACCEPTED MANUSCRIPT

Organism	Carbon source	Cultivation style	Gene	Target product	Target % of total C15 terpenes mad	g CDW /L culture	Target µg/g CDW	Culture time (days)	Target yield µg/L	Total yield µg C15 /L	Target yield µg/L /day	Total C15 yield µg/L/d	Target yield µg/g CDW /da	Total C15 yield µg/g CD
ispA_CFP	**v**	hygromycin B	2465	1701	3	566	62.2	v:**ii**						
ERG20_CFP	**vi**	hygromycin B	2630	1866	3	621	70.8	v:**ii**						
ERG20_PcPs_YFP**	**vii**	paromomycin	4733	3534	6	1177	135.5	v:**i**						
ispA_PcPs_YFP	**viii**	paromomycin	4580	3381	6	1126	127.5	v:**i**						
PcPs_CFP	**ix**	hygromycin B	3384	2475	4	824	94.1	v:**ii**						
PcPs_YFP_PcPs	**x**	paromomycin	5481	4137	7	1378	159.2	v:**i**						
2XPcPs_YFP	**xi**	paromomycin	5487	4143	7	1380	159.4	v:**i**						
3XPcPs_YFP	**xii**	paromomycin	7590	5811	10	1936	223.9	v:**i**						
		UniProt ID												
PcPs alone		Q49SP3	2097	1662	3	554	64.3	KX097887						
CrFPPs alone		A8IX41	3555	1080	11*	360	40.5	-						
ispA alone		P22939	1184	894	2	298	32.0	KX097888						
ERG20 alone		P08524	1346	1056	2	352	40.5	KX097889						

Note: 1 copy of the RBCS2 intron 1 (i1) is found within the HSP70-RBCS2 promoter. In addition, all YFP- or CFP- linked constructs contain the RBCS2i2 intron as part of each fluorescent reporter in the pOptimized vectors, described in Lauersen et al., 2015. Targeted expression of nuclear transgenes in Chlamydomonas reinhardtii with a versatile, modular vector toolkit. Appl. Microbiol. Biotechnol. 99(8) 3491-3503.

*The native FPPs of C. reinhardtii contains 11 natural introns in its genomic sequence (Phytozome v11: Cre03.g207700.t1.1).

**Expressed only as broken constructs identified by YFP fluorescence in this work

Nucleotide sequences for coPcPs, coispA, and coERG20 submitted to NCBI as part of this work.

Table 2. Relative sesquiterpenoid productivities from phototrophic hosts

Accepted manuscript

ACCEPTED MANUSCRIPT

					e							**ay**	**y**	**W/day**
P. patens[1]	Air	50 mL culture, PhyB medium, shake flask	P. cablin patchoulol synthase (PcPs)	patchoulol	0.34	not stated	830	14	-	-	-	-	59	174
			PcPs + tHGMR	patchoulol	0.34	not stated	1,340	14	-	-	-	-	96	282
Synechococcus PCC 7002[2]	1% (v/v) CO_2 in air	100 mL culture, A^+ medium shake flasks	Abies grandis (E)-α-Bisabolene synthase (AgBs)	α-bisabolene	1.00	2.000	300	4	600	600	150	150	75	75
Anabaena sp. PCC 7120[3]	1% (v/v) CO_2 in air	100 mL culture, BG11 medium shake flasks	Picea abies E,E-α-farnesene synthase	α-farnesene	1.00	-	-	15	305	305	20	20	-	-
C. reinhardtii[4]	Acetate	45 mL culture, TAP medium shake flask	PcPs	patchoulol	0.34	0.526	922	6	469	1,379	78	230	154	452
	3% (v/v) CO_2 in air	400 mL culture T2P medium stirred	PcPs	patchoulol	0.34	1.260	279	7	350	1,029	50	147	40	117
	Acetate	400 mL culture TA2P medium stirred	PcPs	patchoulol	0.34	0.700	520	7	363	1,067	52	153	74	218
	Acetate + 3% CO_2	400 mL culture TA2P medium stirred	PcPs	patchoulol	0.34	1.410	309	7	432	1,271	62	183	44	130

[1]Zhan et al. (2014), tHMGR – truncated HMG-CoA reductase from S. cerevisiae, [2]Davies et al. (2014), [3]Halfmann et al. (2014) note biomass only presented as optical density (OD700nm),
[4]This work. C15 denotes total sesquiterpenoids

Accepted manuscript

Highlights

- Expression of Pogostemon cablin patchoulol synthase in Chlamydomonas reinhardtii
- Expression of E. coli ispA and S. cerevisiae ERG20 in C. reinhardtii
- Localization of native FPP synthase in C. reinhardtii
- 223.4 kDa heterologous fusion protein expression in C. reinhardtii
- 1.03 mg L^{-1} phototrophic sesquiterpenoid production from microalgal host

Fig. 1

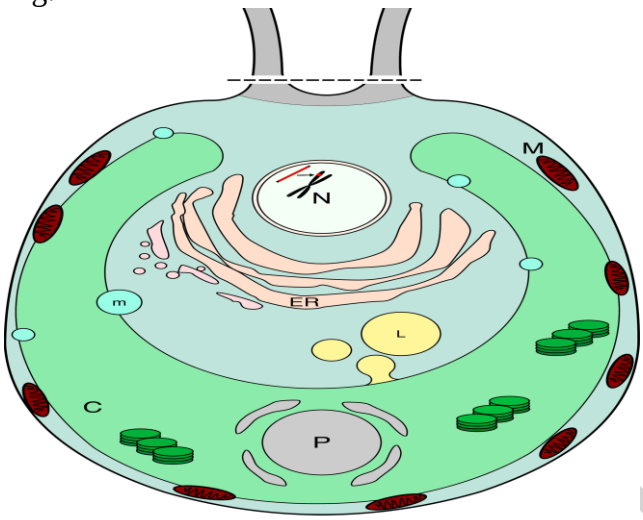

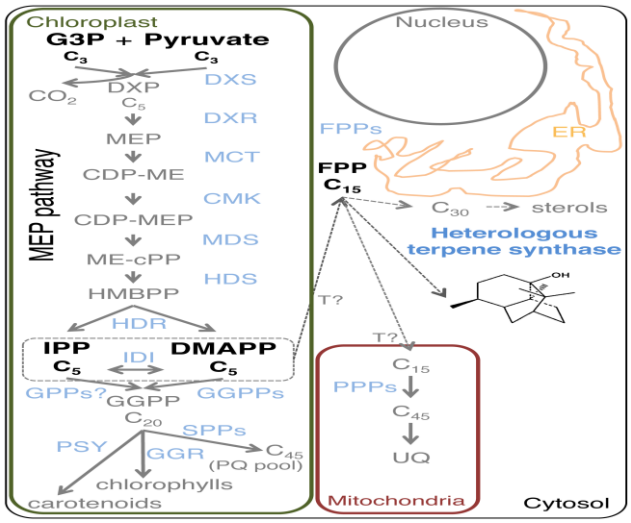

Fig. 2

ACCEPTED MANUSCRIPT

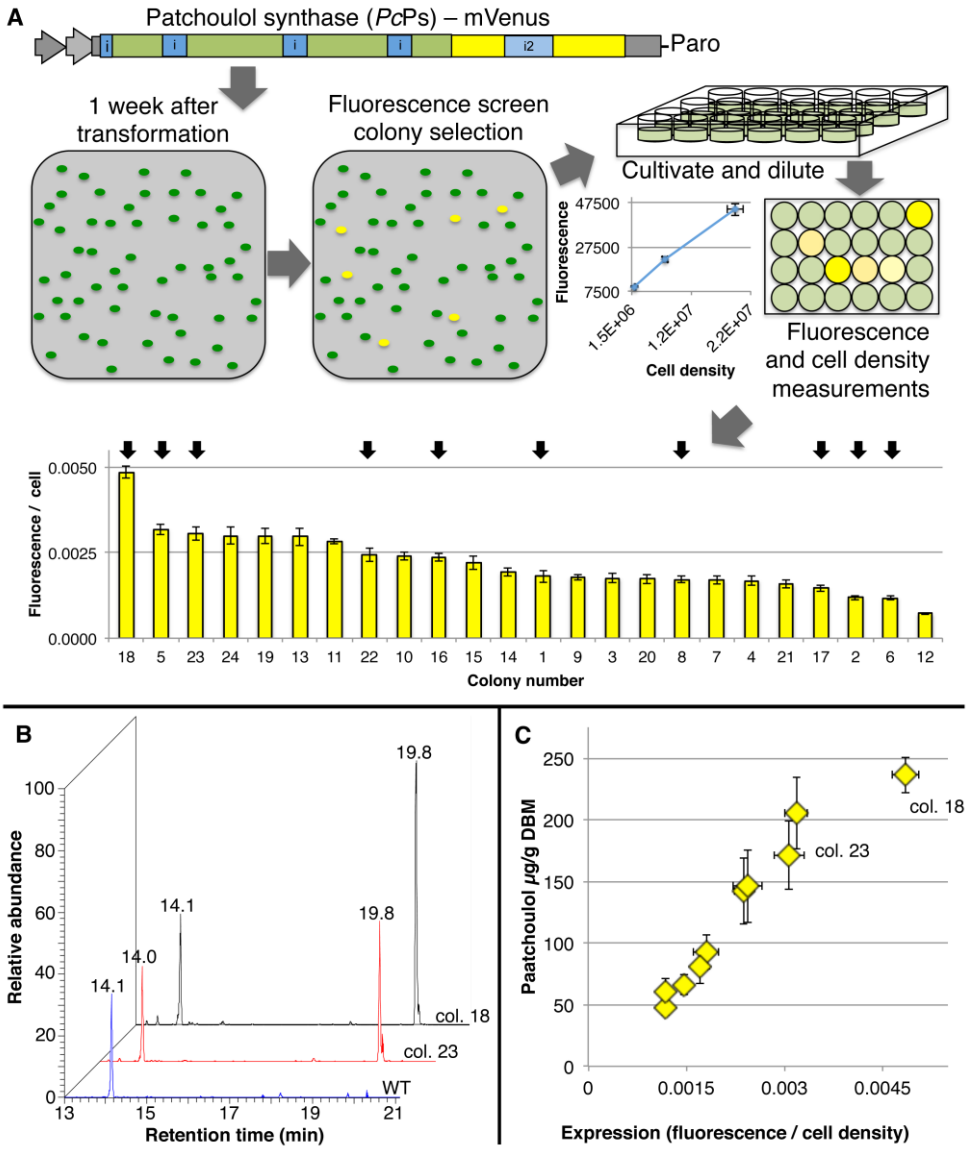

Fig. 3

ACCEPTED MANUSCRIPT

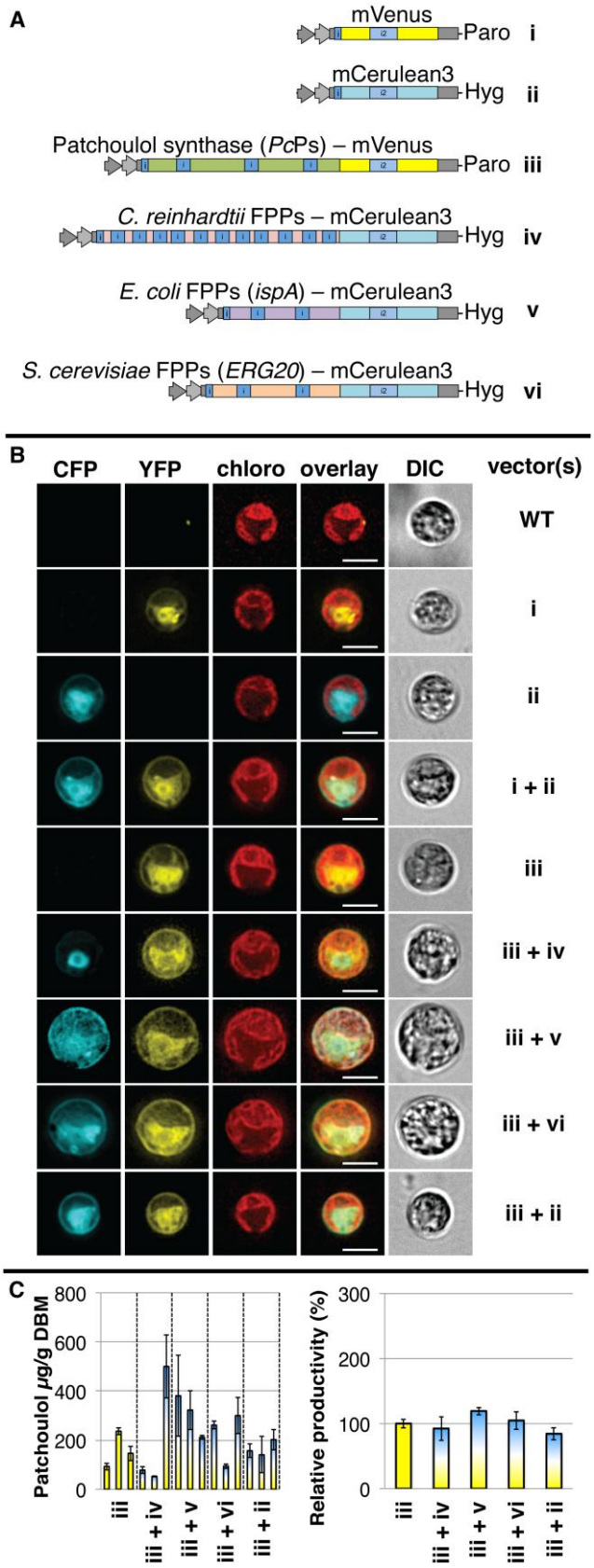

ACCEPTED MANUSCRIPT

Fig. 4

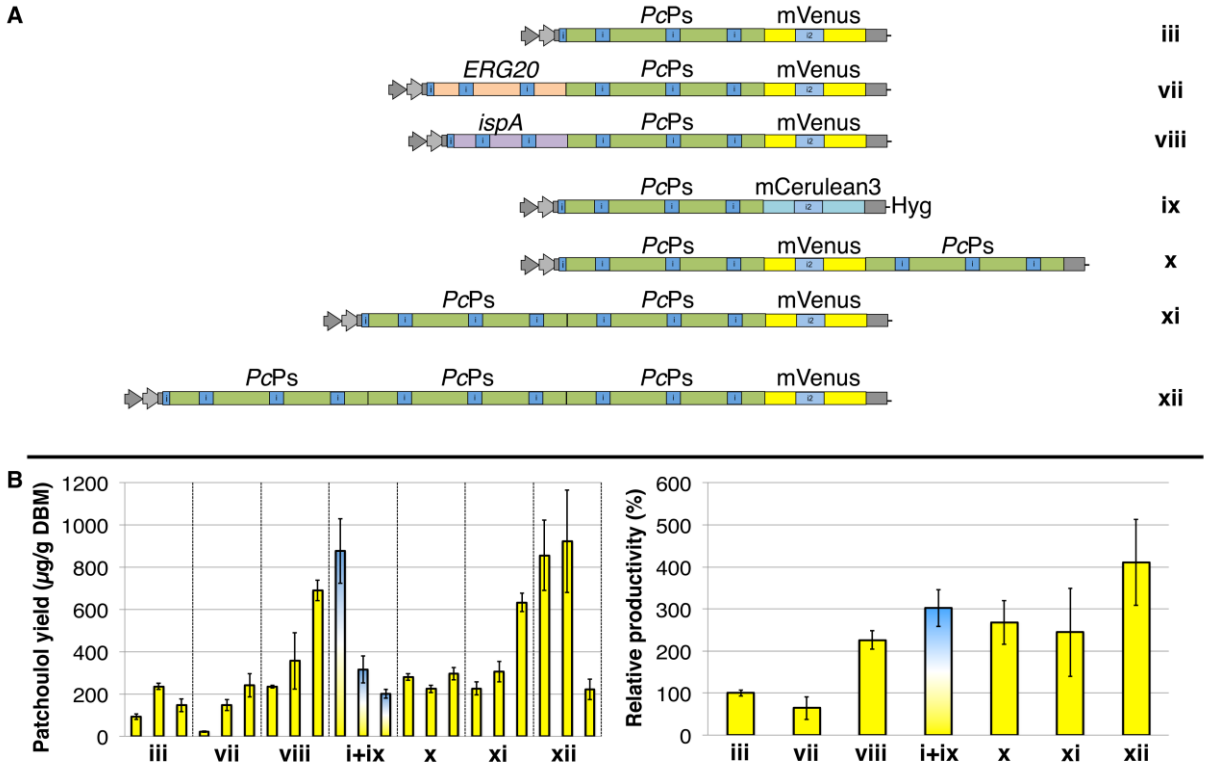

Fig. 5